Howard Hughes Medical Institute

Published as: *Curr Biol*. 2024 September 09; 34(17): 3941–3954.e4.

Light and dopamine impact two circadian neurons to promote morning wakefulness

Jasmine Quynh Le[1], **Dingbang Ma**[1,2], **Xihuimin Dai**[1], **Michael Rosbash**[1,3,*]

[1]Howard Hughes Medical Institute and Department of Biology, Brandeis University, Waltham, Massachusetts 02453, USA

[2]Interdisciplinary Research Center on Biology and Chemistry, Shanghai Institute of Organic Chemistry, Chinese Academy of Sciences, Shanghai 201210, China

[3]Lead Contact

Summary

In both mammals and flies, circadian brain neurons orchestrate physiological oscillations and behaviors like wake and sleep; these neurons can be subdivided by morphology and by gene expression patterns. Recent single-cell sequencing studies identified 17 *Drosophila* circadian neuron groups. One of these includes only two lateral neurons (LNs), which are marked by the expression of the neuropeptide ion transport peptide (ITP). Although these two ITP$^+$ LNs have long been grouped with five other circadian evening activity cells, inhibiting the two neurons alone strongly reduces morning activity, indicating that they also have a prominent morning function. As dopamine signaling promotes activity in *Drosophila* like in mammals, we considered that dopamine might influence this morning activity function. Moreover, the ITP$^+$ LNs express higher mRNA levels than other LNs of the type 1-like dopamine receptor Dop1R1. Consistent with the importance of Dop1R1, cell-specific CRISPR/Cas9 mutagenesis of this receptor in the two ITP$^+$ LNs renders flies significantly less active in the morning, and *ex vivo* live imaging shows Dop1R1-dependent cAMP responses to dopamine in these two neurons. Notably, the response is more robust in the morning, reflecting higher morning Dop1R1 mRNA levels in the two neurons. As mRNA levels are not elevated in constant darkness, this suggests light-dependent upregulation of morning Dop1R1 transcript levels. Taken together with the enhanced morning cAMP response to dopamine, the data indicate how light and dopamine promote morning wakefulness in flies, mimicking the important effect of light on morning wakefulness in humans.

*Correspondence: rosbash@brandeis.edu.

Author Contributions

Conceptualization, J.Q.L., D.M. and M.R.; Methodology, J.Q.L. and M.R.; Validation, J.Q.L., X.D.; Formal Analysis, J.Q.L.; Investigation, J.Q.L; Resources, J.Q.L, D.M., X.D.; Data Curation, D.M.; Writing – Original Draft, J.Q.L.; Writing – Review & Editing, X.D., M.R.; Visualization, J.Q.L; Supervision, M.R., Project Administration, M.R.; Funding Acquisition, M.R.

Declaration of Interests

The authors declare no competing interests.

eTOC Blurb

Light and dopamine generally enhance wakefulness. Le et al. use single-cell RNA sequencing data, transgenic manipulations, and *ex vivo* live imaging to characterize two discrete circadian neurons. These neurons specifically increase wakefulness in the morning through enhanced type-1 like dopamine receptor activity around the onset of light.

Keywords

Circadian neurons; activity; sleep; dopamine; Dop1R1; cAMP; Drosophila

Introduction

Wake and sleep are regulated by both a circadian and a homeostatic process.[1] The latter monitors the duration an animal has been awake and the accumulation of sleep debt, whereas the 24-hour circadian drive determines when this sleep debt can be discharged. When circadian drive is high and sleep debt is low, animals transition more easily to wake. The detailed interactions between these two processes in driving circadian behavior remain unclear.

Circadian drive is usually reset each day by light. In mammals including humans, the light signal is passed from the retina to the suprachiasmatic nucleus (SCN) in the hypothalamus via the retinal-hypothalamic track. The SCN is considered the master clock and the most important circadian pacemaker in mammals.[2] Additionally, light reduces sleep inertia, the phenomenon that describes grogginess upon transitioning to wake.[3] Studies have also shown that premature light, illumination before scheduled waking, reduces sleep inertia.[4,5] This is the case when we experience early morning sunlight during summertime or simulated dawn with artificial lights.

The circadian and homeostatic processes collaborate to craft the stereotyped bimodal activity pattern of *Drosophila melanogaster*, which peaks in the morning around the onset of dawn (or lights-on) and again in the evening around the onset of dusk (or lights-off). This activity pattern is dependent on an important subset of the 150 circadian neurons, the 15 pairs of lateral neurons (LNs) that are symmetrically present on both sides of the brain. They comprise of both morning cells and evening cells, which regulate locomotor activity in the morning and in the evening, respectively.[6,7]

The morning cells comprise of eight pairs of ventrally-located lateral neurons (LN_vS), four large LN_vs (lLN_vs) and four small LN_vs (sLN_vs). The lLN_vs contact the medulla of the optic lobes, where they receive light input,[8] and the sLN_vs regulate rhythmicity in constant darkness.[9] All eight LN_vs express the neuropeptide pigment dispersing factor (PDF), which synchronizes the activity of many other circadian neurons.[10]

The seven pairs of neurons that have traditionally been considered evening cells consist of six dorsolateral neurons (LN_ds) and one remaining sLN_v; the latter cell is PDF-negative and also known as the 5^{th} sLN_v. However, whether all LNds affect only the evening and not the morning locomotor activity peak has been questioned.[11,12] Relevant to this possibility is

the fact that the 5th sLNv and three of the six LN_ds are sensitive to PDF from the morning cells. This is because these four cells express the PDF receptor (PDFR).[13] They are also light sensitive as they express the blue light-sensitive circadian protein CRYPTOCHROME (CRY), which is required by evening cells for light entrainment.[14] The remaining three LN_ds are both $PDFR^-$ and CRY^-.[15]

This substantial heterogeneity in evening cell gene expression is mirrored by a comparable heterogeneity in neuropeptide expression. Two of the CRY^+ LN_ds express both the short neuropeptide F (sNPF) and Trissin,[16] whereas the third CRY^+ LN_d expresses the neuropeptide NPF.[17,18] Two CRY^- LN_ds also express NPF as does the 5th sLN_v.[17,18] The 5th sLN_v as well as one CRY^+ LN_d also express the neuropeptide ion transport peptide (ITP).[19,20] The ITP^+ sLN_v and ITP^+ LN_d (ITP^+ LNs) contribute to the regulation of the evening locomotor activity peak.[18,20]

Recent electron microscopy (EM) connectome data highlights a comparable heterogeneity in evening cell connectivity.[21–24] LN_ds can be categorized into three groups based on shared connectivity patterns, two CRY^+ groups and one CRY^-. One of these CRY^+ groups contains the two ITP^+ LNs, which share strong synapses with each other,[22] suggesting shared functions.

This dramatic heterogeneity parallels our previous characterization of circadian neuron transcriptomes at different clock times using bulk and single-cell RNA sequencing.[16,25,26] The more recent single-cell RNA sequencing datasets used an unsupervised clustering method to identify high-confidence molecular subtypes with marker genes that match known identifiers of subtypes, such as G-protein coupled receptors and neuropeptides.[16,26] This extensive dataset sits alongside years of immunohistochemistry work from various labs and underscores the molecular diversity of the evening neurons.

With a focus on understanding how these seven circadian neurons regulate sleep and wake, we investigated how they are affected by the arousal signal dopamine. Previous studies indicated that dopamine stimulates morning cell activity, specifically the ILN_vs, which respond to dopamine through increases in cAMP signaling. Light suppresses this response by upregulating the inhibitory dopamine receptor Dop2R.[27] Another study found that dopamine signaling to the ILN_vs is mediated by the dopamine receptor Dop1R1 and suggested that another dopamine receptor Dop1R2 present on the sLN_vs promotes nighttime sleep.[28] In yet another recent study, we showed that dopamine enhanced sleep through yet another circadian neuron group, the DN1s.[29] However, a link between dopamine and the important wake-promoting evening cells has not been established. We were also encouraged to focus on the ITP^+ LNs in the context of sleep and wake because a genetic intersection strategy combined with other data shows that they are upstream of the other evening cells.

Indeed, optogenetic activation of novel and highly specific split-GAL4 lines indicates that the two ITP^+ LNs can promote wakefulness by reducing sleep pressure and sleep depth. Relevant to dopamine, these cells express the wake-affiliated dopamine receptor Dop1R1 and CRISPR/Cas9-mediated mutation of this receptor in only the ITP^+ LNs significantly decreases morning activity. Since the Dop1R1 knockout primarily increases sleep depth,

this suggests that dopamine signaling to these ITP$^+$ LNs serves to decrease sleep depth and promote wakefulness in the morning. Consistent with this notion, *ex vivo* live imaging of cAMP in ITP$^+$ LNs confirms that dopamine signaling to these neurons is mediated by Dop1R1. These results not only reveal an unexpected function of the ITP$^+$ LNs, specifically their role in regulating wake and sleep in the morning, but also shed light on a new dopaminergic signaling pathway within the circadian network.

Results

ITP-expressing lateral neurons top the evening cell connectomic hierarchy

The evening cells are implicated in promoting the locomotor activity peak towards the end of the daytime and include six LN$_d$s and one sLN$_v$. Using the publicly available NeuPrint hemibrain and FlyWire whole brain electron microscopy connectome datasets,[21,23,24,30] we compared connection strengths among all evening cells in two adult female *Drosophila* brains. The hemibrain connectome displays one set of evening cells (Figure 1A, left), while the FlyWire whole brain connectome shows two sets—one from each brain hemisphere (Figure 1A, right).

Despite variations in the number of synapses between connectomes and even between hemispheres of the whole brain connectome, three consistent themes emerged across all three sets of evening cells. First, the ITP-expressing sLN$_v$ and ITP-expressing LN$_d$ (ITP$^+$ LNs) exhibit strong interconnections, surpassing all connections with any other evening cells. Second, the ITP$^+$ LNs synapse onto only two other evening cells, the two Trissin-expressing LN$_d$s (Trissin$^+$ LN$_d$s). Notably, this connection is not reciprocated (Figure 1B), which reinforces this top-down view. Third, we did not observe any robust synaptic connectivity between the ITP$^+$ LNs and the remaining three LN$_d$s using a threshold of five synapses to define a valid connection. However, there are weak sub-threshold unidirectional connections from the ITP$^+$ sLN$_v$s and from one Trissin$^+$ LN$_d$ to the remaining CRY$^-$ LN$_d$s based on the NeuPrint hemibrain dataset.[22] In summary, the synaptic weights and directions within all evening cells strongly suggest that the ITP$^+$ LNs sit at the top of this circadian neuron group.

To provide finer detail in morphologically characterizing the ITP$^+$ LNs, we employed a method that utilizes fluorescent labeling at the intersection of a GAL4 line and a LexA line (Figure S1A). By utilizing *Clk856-GAL4*[31] to express a flippase-dependent fluorescent reporter *UAS-FRT-STOP-FRT-mVenus* in nearly all circadian neurons and an *ITP-LexA* knock-in line[32] with *LexAop-flippase* to express flippase in all ITP-expressing neurons, we identified two neurons marked by both driver lines. Co-staining with an antibody for the circadian protein Period (PER) confirmed that a single LN$_d$ and a single sLN$_v$ are the only ITP$^+$ circadian neurons (Figure S1B), consistent with previous ITP antibody staining findings.[20] Notably, the ITP$^+$ LN$_d$ not only projects to the dorsal region of the brain but it also projects to the accessory medulla (AMe), unlike other evening cells. This is a key circadian region located at the anterior of the brain. It contains the LN$_v$s and receives inputs from the eyes.[33–36]

Additionally, the axonal projection to the AMe from the ITP$^+$ LN$_d$ has a distinctive axonal bifurcation feature (Figure S1B, center, white arrowhead), which is absent in the other LN$_d$s (Figure S1C, right). The bifurcation is also evident in EM reconstructions of the ITP$^+$ LN$_d$ (Figure S1C, center) but not in other evening cells (Figure S1C, right) or the ITP$^+$ sLN$_v$ (Figure S1C, left). This bifurcation allows for confident morphological distinction of the ITP$^+$ LNd from other evening cells.

ITP$^+$ LNs are wake-promoting circadian neurons

Given the distinct molecular, morphological, and connectomic features of the ITP$^+$ LNs, we asked whether these two neurons alone could influence circadian locomotor activity and sleep. To gain transgenic access to these neurons, we screened expression patterns of Janelia split-GAL4 driver lines from the Rubin Lab with the fluorescent protein expressed from *UAS-EGFP*. We looked for a driver line exhibiting the characteristic axonal bifurcation of the ITP$^+$ LNd and identified a novel split-GAL4 driver line, *ss00639-GAL4* (Figure 2A): it only labels the two ITP$^+$ LNs with few extra PER$^-$ and CRY$^-$ cells.[37] There is also the *MB122B-GAL4*[38] line, which labels the two ITP$^+$ LNs and two other circadian neurons, the Trissin$^+$ LNds (Figure S2D).

We then expressed a red light–sensitive channelrhodopsin, *UAS-CsChrimson*,[39] together with *ss00639-GAL4* to be able to optogenetically activate the ITP$^+$ LNs with red light. The two parental lines with heterozygous expression of GAL4 and UAS alone were used as controls. A free-standing video-recording setup, FlyBox,[38] was used to observe locomotor and sleep behavior of these flies under standard 12:12 light-dark conditions (LD) and delivered optogenetic stimulation.

During 12:12 LD baseline conditions, control flies and experimental flies expressing CsChrimson in the ITP$^+$ LNs exhibited similar activity and sleep levels (Figure 2B, left panels). During 24 hours of red light stimulation however, experimental flies had dramatically higher activity levels and reduced sleep (Figure 2B, right panels) compared to control flies. Both control lines were unaffected by red light during the daytime, whereas optogenetically activated experimental flies lost most of their daytime sleep. Although control flies were woken by the stimulating red light during the nighttime, flies with both transgenes were much more active and had much lower nighttime sleep. This suggests that optogenetic activation of the ITP$^+$ LNs promotes activity much more strongly than white light alone. Closer inspection of sleep structure during the daytime indicated ITP$^+$ LNs activation increases the probability of sleeping flies waking up (p-wake) and decreases the probability of awake flies falling asleep (p-doze) during ZT00-06 and ZT06-12 (Figure 3C).[40]

We next tested whether the Trissin$^+$ LN$_d$s are activity-promoting like the ITP cells. Because we did not have a Trissin-only LN$_d$ line, we activated these two neurons using an intersectional strategy. *Clk856-GAL4* labels all LNs and other circadian neurons, so we combined this GAL4 line with *UAS-FRT-STOP-FRT-CsChrimson*,[41] *LexAop-flippase*, and a *Trissin-LexA* knock-in line[32] to label only the two Trissin$^+$ LN$_d$s (Figure S2A). There was no change in activity, sleep, p-wake, nor p-doze observed when compared to heterozygous genetic controls (Figure S2B–C). However, activating both the ITP$^+$ LNs and the Trissin$^+$

LN_ds with *MB122B-GAL4* (Figure S2D) resulted in a significant increase in activity and decrease in sleep (Figure S2E) similar to the effect with *ss00639-GAL4* shown above. With *MB122B-GAL4*, p-wake and p-doze are affected during ZT00-06 and not during ZT06-12 (Figure S2F). These data collectively indicate that the ITP^+ LNs are wake-promoting but that the $Trissin^+$ LN_ds are not.

Inhibiting ITP^+ LNs decreases morning wakefulness

To complement the above activation experiments, we silenced the ITP^+ LNs with two independent approaches: expressing the inward rectifying K^+ channel Kir2.1 with *UAS-Kir2.1*[42] and expressing tetanus toxin (TNT) with *UAS-TNT*[43] to block neurotransmitter release with *ss00639-GAL4*.

Silencing with *UAS-Kir2.1* decreased activity and increased sleep during the daytime, particularly between ZT00 and ZT06, compared to heterozygous genetic controls (Figure 3A–B). P-wake is decreased between ZT00 and ZT06, whereas the change in p-doze is not significant in compared to both heterozygous genetic controls (Figure 3C). The results were very similar with *UAS-TNT* (Figure 3D–F). Both inhibition methods also caused a small decrease in the evening activity peak compared to controls, aligning with previous reports on evening cell inhibition[18,20,44] although the effect is statistically significant with TNT, but not Kir2.1 (Figure 3B, E). Consistent results were also observed with silencing and blocking neurotransmission of both ITP^+ LNs and $Trissin^+$ LN_ds using *MB122B-GAL4* (Figure S3A–F). These findings further underscore the activity-promoting role of the two ITP^+ LNs after the onset of light and focused our attention on the morning, particularly between ZT00 and ZT06, as well as the more expected effect on the evening activity peak.

ITP^+ LNs express higher levels of *Dop1R1* in the morning

Because the activation of different subsets of dopaminergic neurons has been demonstrated to promote wakefulness in *Drosophila*,[45] we considered dopamine as a good candidate for an upstream arousal molecule. Moreover, our single-cell RNA sequencing data of circadian neurons[16] showed that most circadian neurons express transcripts encoding a variety dopamine receptors (Figure 4A). For example, Dop1R1 and DopEcR are broadly expressed in circadian neurons, whereas Dop1R2 is limited to only a few clusters. The inhibitory receptor Dop2R is expressed at low levels in most clusters but more highly expressed in specific clusters. Expression within evening cells is visualized more easily by examining circadian time points in more detail. Dop1R1 and Dop2R show similar expression levels across all evening cells, while Dop1R2 is either absent or expressed at very low levels in all clusters (Figure S4A–C). DopEcR expression levels are high but variable in evening cells, consistent with other circadian neurons (Figure S4D).

The ITP^+ LNs are recognizable through their notably high ITP expression (Figure 4B). These two cells express Dop1R1 prominently, along with some Dop2R and DopEcR, while virtually lacking Dop1R2 expression (Figure 4A). Intriguingly, Dop1R1 mRNA in the ITP^+ LNs follows a cycling pattern with a peak in the morning at ZT02 (Figure 4C). Intriguingly, this is the only evening cell cluster and dopamine receptor for which morning expression is

decreased in constant darkness, indicating a special relationship between light, the ITP$^+$ LNs and Dop1R1 (Figure S4A).

Functional knock-out of Dop1R1 in ITP$^+$ LNs decreases morning wakefulness

Because of the morning sleep/activity effect of activation and inhibition shown above, we further pursued the contribution of dopamine and Dop1R1 to the two ITP$^+$ LNs. To this end, we employed a CRISPR/Cas9 mutagenesis method[29,37,46] to specifically knock out Dop1R1 function in wake-promoting ITP$^+$ LNs. Given that Dop1R1 is known as an excitatory dopamine receptor,[47] our hypothesis was that knocking out Dop1R1 in these neurons would diminish their activity, leading to reduced wake-promotion throughout the day. However, the results revealed a decrease in activity and an increase in sleep only in the morning, specifically between ZT00 and ZT06 under standard 12:12 LD conditions (Figure 5A–B). Importantly, activity and sleep levels remained indistinguishable from the control strains thereafter. Similar effects were observed with RNAi knock-down of Dop1R1 in these neurons (Figure S5C, black arrowheads). Given that ITP$^+$ LNs are a subset of the evening cells responsible for regulating the evening activity peak,[18,20,44] the unchanged evening activity anticipation and peak with Dop1R1 knock-out in these cells indicates a dedicated contribution of these cells, their Dop1R1 expression and dopamine to morning wakefulness.

The decrease in morning wakefulness can result from either a stronger drive towards sleep and/or a decreased wake drive. Examining sleep structure indicated that the decrease is due to both, a significant decrease in p-wake and an increase in p-doze between ZT00 and ZT06 compared to the control strains (Figure 5C). In contrast, the difference in the second half of the daytime, during ZT06 and ZT12 was more variable and not significant. Although activity and sleep were similarly affected with CRISPR/Cas9 knock-out (Figure S5A–B) and RNAi knock-down (Figure S5D, black arrowheads) in ITP$^+$ LNs and Trissin$^+$ LN$_d$s with *MB122B-GAL4*, p-wake was significantly decreased between ZT00 to ZT06 while p-doze did not significantly differ from both controls (Figure S5C). These findings suggest that dopamine inputs to Dop1R1 in ITP$^+$ LNs typically create a strong drive towards wakefulness by decreasing morning sleep depth after the onset of light.

Dopamine increases cAMP levels in ITP$^+$ LNs

Given the significance of Dop1R1 function in ITP$^+$ LNs for morning wakefulness, we examined the cellular effects of dopamine on these neurons using an intracellular cAMP sensor, EPAC-H187[48]. We cloned this sensor into flies under UAS control[49] and expressed it in ITP$^+$ LNs using *ss00639-GAL4*. Live cAMP changes in response to dopamine were recorded in whole brain explants using confocal microscopy. To minimize network effects, brains were incubated in adult hemolymph-like saline (AHL) with tetrodotoxin (TTX) for at least five minutes before recording to inhibit polysynaptic inputs; all experiments were conducted with TTX. One minute of baseline activity was recorded before perfusing each brain with dopamine and with forskolin directly afterwards as a positive control.

In both the ITP$^+$ LN$_d$ and the ITP$^+$ sLN$_v$, we observed increases in cAMP in response to 400 μM dopamine and 50 μM forskolin (Figure S6A–B, blue traces). To confirm that the response to dopamine is mediated by Dop1R1, we co-expressed our sensor *UAS-EPAC-*

H187 and the Dop1R1-guides (with *UAS-Cas9.P2*) in *ss00639-GAL4* to measure the cAMP response to dopamine without functional Dop1R1 receptors. There were no responses to dopamine in either the ITP$^+$ sLN$_v$ or the ITP$^+$ LN$_d$ with the knock-out (Figure S6A–B, orange traces), indicating that the cAMP response is indeed driven through the Dop1R1 receptors. Importantly, both cells still responded to forskolin, showing that they can still mount a cAMP response through other pathways.

We hypothesized that cAMP responses to dopamine would be more pronounced during the light phase around ZT02 when *Dop1R1* mRNA levels are highest compared to the dark phase when *Dop1R1* mRNA levels are lowest (Figure 4C). To capture time-of-day differences in cAMP responses, we utilized unpublished 10XUAS versions of newly available and more sensitive EPAC sensors called cAMPFIRE.[50]

Responses to 100 μM dopamine and 50 μM forskolin were observed during the light phase between ZT01 and ZT03 and the dark phase between ZT13 and ZT15 in both ITP$^+$ LNs with these *10XUAS-cAMPFIRE* sensors (Figure 6A–B). However, the robustness of the response, defined as how quickly the response rises, was significantly greater in the light phase than in the dark phase in the ITP$^+$ sLN$_v$ (Figure 6C). (The slopes are described in the legend of Figure 6A–B.) The response in the ITP$^+$ LN$_d$ also trended higher during the light phase, but the difference with the dark phase was not statistically significant. The data indicate that the single ITP$^+$ sLN$_v$ may play a more substantial role than the ITP$^+$ LN$_d$ in dopaminergic modulation of morning wakefulness and suggest that the cycling of *Dop1R1* mRNA levels within these cells contributes to the control of time-of-day wakefulness.

Optogenetic inhibition of ITP$^+$ LNs decreases morning wakefulness on the subsequent day

To achieve acute inhibition, we optogenetically inhibited the ITP$^+$ LNs by expressing the green light-sensitive channelrhodopsin *UAS-GtACR1* with *ss00639-GAL4*. The two parental lines with heterozygous expression of GAL4 and UAS alone were used as controls. FlyBox was used to observe locomotor and sleep behavior of these flies under standard 12:12 LD and to deliver optogenetic stimulation.

During 12:12 LD baseline conditions, control flies and experimental flies expressing *GtACR1* in the ITP$^+$ LNs exhibited similar activity and sleep levels (Figure 7A, left panels). During 24 hours of green light stimulation, experimental flies had a substantially reduced evening activity peak and slightly more sleep, whereas control flies were unaffected during the beginning of the day, but had a broadened evening peak (Figure 7A, middle panels) compared to the baseline day. This broadening is due to extended light exposure in the dark. There was no effect on morning wakefulness during acute inhibition. However, activity was greatly reduced and sleep was increased in the morning between ZT00 and ZT06 on the subsequent recovery day (Figure 7A, right panels) in the experimental flies, similar to the chronic inhibition effects shown above (Figure 3). The controls do not manifest this same response, which further highlights the distinct role that the ITP$^+$ LNs have in regulating morning wakefulness and suggests separate control over morning and evening sleep. This is because all three strains exhibit substantially reduced evening activity on the subsequent recovery day, which could reflect evening rebound sleep in response to sleep loss from nighttime green light exposure.

We assayed sleep structure during the green light inhibition and found a significant decrease in p-wake within the broadened activity peak between ZT12 and ZT18 in the experimental flies compared to the controls (Figure 7B, left); there was no change in p-doze (Figure 7B, right). When assessing the change in sleep structure during the recovery day in comparison to the baseline day, we observed a significant decrease in p-wake and significant increase in p-doze in the morning between ZT00 and ZT06 (Figure 7C). These results indicate that neuronal activity of the ITP^+ LNs rapidly affects the evening peak, perhaps directly, whereas the effect on morning wakefulness is slower and may require ITP^+ LN neuronal activity before the morning activity effect is manifest.

Discussion

Although the circadian evening neurons have been shown to be activity-promoting,[6,38] there is little information that distinguishes the function(s) of one cell from another. To this end, we began by identifying and comparing the connectivity patterns of these seven neurons. The two ITP^+ LNs emerged at the top of a hierarchy, hinting that they may have a special and important role. Subsequent identification of split-GAL4 lines for labeling ITP^+ LNs showed that they promote wake at all times of day, but inhibition of these neurons indicated that they contribute to morning wakefulness as well as their more expected contribution to evening activity. Single-cell RNA sequencing showed that *Dop1R1* mRNA is more highly expressed in the ITP^+ LNs than in other LNs. Dopamine also induces increased cAMP levels within these neurons, which is more pronounced during the day than the night. Furthermore, *Dop1R1* mRNA levels in ITP^+ LNs are highest in the morning during light-dark conditions but not constant darkness, which suggests that light-dependent cycling of Dop1R1 contributes to their morning arousal function.

Although the ITP^+ LNs emerged as prominently interconnected as well as connected to other evening cells, this relationship was unidirectional. There were almost no pre-synaptic connections from the other evening cells to the ITP^+ LNs at the particular time-points examined. This conclusion was drawn after analyzing two EM connectome datasets and builds upon earlier studies that primarily addressed inter-LN_d connections.[22] In addition, the morphological distinctions between the four LN_d subtypes we identified was consistent with extensive prior research that classified LN_ds based on their protein and RNA expression.[15,16,19]

The two ITP^+ LNs have robust synaptic connections with the two $Trissin^+$ LN_ds (Figure 1A), which are a second evening cell subtype and are located directly downstream of the ITP^+ LNs. These $Trissin^+$ LN_ds are included in the expression pattern of *MB122B-GAL4* along with the two ITP^+ LNs. Exciting neurons with this driver had very similar effects to exciting only the two ITP^+ LNs with *ss00639-GAL4*, i.e., a large increase in activity (Figure 2B and S2E). The only difference between these two drivers is that *MB122B-GAL4* activation increases p-wake between ZT00 to ZT06 and not between ZT06 to ZT12 (Figure S2F), suggesting that the $Trissin^+$ LN_ds have an inhibitory effect in the latter timespan. However, directly activating only the $Trissin^+$ LN_ds, (Figure S2C) did not change activity or sleep during any timespan. In any case, these data also suggest that the wake-promoting effect of *MB122B-GAL4* is due to the ITP^+ LNs and not the $Trissin^+$ LN_ds.

Although the ITP$^+$ LNs are clearly wake-promoting when activated, the effect of chronic inhibition with two different methods as well as optogenetic inhibition was much more discrete. Optogenetic activation may therefore induce “ectopic” effects by virtue of excessive neuronal activity and/or bypassing normal time of day regulation. Enhanced activity of the ITP$^+$ LNs could be activating cells that are less active under normal conditions. The could include other evening cells, which is consistent with the connectomic data (Figure 1). The large decrease in the evening peak during 24-hour optogenetic inhibition (Figure 7) indicates that this evening peak effect is independent of development and consistent with the large body of evidence that the LN$_d$s are evening cells as described above.

The optogenetic inhibitory effect also rules out development as necessary for the morning wakefulness effect (Figure 7). Moreover, the lack of an acute morning effect is consistent with evidence that Ca^{2+} levels of evening cells peak in the evening, around ZT12 in LD and ZT08/09 in DD.[51,52] Taken together with the chronic inhibition results (Figure 3), the delayed effect of optogenetic inhibition on morning wakefulness suggests that gene expression changes and more sustained ITP+ LN activity may be necessary for morning wakefulness. *Dop1R1* mRNA is an attractive target of this activity. Chronic or sustained inhibition may be required to reduce Dop1R1 levels within ITP$^+$ LNs, i.e., acute inhibition starting at ZT00 is not sufficient for any substantial effect on Dop1R1 levels in the morning. In any case, an attractive model for the morning effect is that ITP$^+$ LN evening activity and subsequent morning light together is required for the upregulation of *Dop1R1* mRNA, which is essential for this observed morning wakefulness effect.

Notable in this context are the temporal dynamics of *Dop1R1* transcript expression, which has a morning peak in the ITP$^+$ LNs (Figure 4C). Because *Dop1R1* is more expressed in ITP$^+$ LNs compared to other evening cells (Figure S4), we considered dopamine as a good candidate for a relevant upstream morning molecule. To address this possibility, we used CRISPR/Cas9 to knock out *Dop1R1*. This caused a substantial loss of wakefulness and increased sleep during the morning hours, notably between ZT00 and ZT06 (Figure 5A), which resembled the effect of neuronal inhibition. This sleep increase was predominantly due to a reduced likelihood of spontaneously awakening from a sleep state (Figure 5B), indicating that Dop1R1 plays a prominent role in enhancing morning arousal. This finding is concordant with prior studies demonstrating the wake-promoting effects of dopaminergic neurons.[45,53]

The literature indicates that the impact of dopamine on the *Drosophila* circadian network is more complicated than its focused effect described here. Dopamine also enhances locomotor activity through its effect on lLN$_v$s,[27] and it has been reported to promote rather than inhibit sleep through its action on sLN$_v$s and DN1s.[28,29] Nonetheless, it is hard to ignore the similar effects of inhibition and Dop1R1 knockout; both indicate that the ITP$^+$ LNs promote morning arousal.

This period of time, between ZT00-ZT06, is not normally associated with evening cell activity.[51,52] This recalls the fact that the ITP$^+$ LN$_d$ cell is the only evening neuron to project to the AMe, where the PDF$^+$ LN$_v$s morning cells reside. The other ITP$^+$ LN is the single

PDF$^-$ sLN$_v$. Its cell body resides within the AMe adjacent to the PDF$^+$ LN$_v$s, i.e., both ITP$^+$ LNs are well-positioned to communicate directly with morning cells. It is notable that the ITP$^+$ LN projections to the AMe are dendritic as well as synaptic, suggesting that the AMe can be an input as well as an output region of these cells.[54] Additionally, forced depolarization of the ITP$^+$ LNs and the Trissin$^+$ LN$_d$s together has been shown to elicit an excitatory response in the PDF$^+$ sLN$_v$s.[55] The ITP$^+$ LNs could therefore enhance morning cell activity, and/or the morning cells could influence the ITP$^+$ LNs, which express PDFR.[15]

The substantial cycling of *Dop1R1* mRNA levels in light-dark (LD) conditions is largely absent by four days in constant darkness (DD) (Figure S4). Intriguingly, the ITP$^+$ LNs are the only evening cell cluster and *Dop1R1* mRNA is the only dopamine receptor transcript for which mRNA expression is decreased in DD, suggesting a special relationship between light and Dop1R1 gene expression within the ITP$^+$ LNs (Figure S4A). Indeed, the ITP$^+$ 5th sLNv responds to light most strongly, and the ITP$^+$ LN$_d$ the third strongest compared to other circadian neurons.[36] Similarly, the ITP$^+$ 5th sLNv has a more robust cAMP response to dopamine than the ITP$^+$ LN$_d$ (Figure 6). The fact that cAMP affects gene expression is consistent with the much slower timescale of the morning wakefulness response to acute firing.

Although we have at present no mechanistic explanation for the light-mediated upregulation of *Dop1R1* mRNA levels in only these two neurons, a likely teleological explanation for this relationship is that light and dopamine amplify circadian morning wake-drive. This emphasizes the extent to which these two circadian neurons and their discrete behavioral output are sensitive to environmental conditions (light) as well as possibly internal state (dopaminergic tone). This relationship may also serve as a possible model for humans experiencing less sleep inertia, more wake-drive, with light exposure, either from early morning sun or from simulated dawn with artificial light before an alarm.[4,5]

Although the cycling of *Dop1R1* mRNA levels is based on RNA sequencing data, the more robust dopamine-mediated cAMP response from daytime than from nighttime brains suggests that *Dop1R1* protein levels and activity in the two ITP$^+$ LNs are also higher in the daytime than the nighttime. This is the first indication that the cycling of GPCR mRNA levels[16,25,29] is of functional significance. Notably, the cycling of *Dop1R1* RNA levels and protein/activity levels are likely not identical in the two neurons, a possibility that is supported by the larger sLN$_v$ day-night difference than LN$_d$ day-night difference in response to dopamine perfusion. This suggests higher *Dop1R1* activity and perhaps a bigger morning arousal role for the ITP$^+$ sLN$_v$ than the ITP$^+$ LN$_d$. This distinction also serves as a reminder that even a two cell-cluster may harbor internal heterogeneity. More generally put, even the considerable cell type complexity of the fly brain circadian neuron system[16,22] is likely to be an underestimate: every circadian neuron may be discrete, at the transcriptomic and anatomical level and perhaps even at the functional level.

RESOURCE AVAILABILITY

Lead contact

Further information and requests for resources and reagents should be directed to and will be fulfilled by the Lead Contact, Michael Rosbash (rosbash@brandeis.edu).

Materials availability

Fly stocks generated in this study are available at Brandeis University.

Data and code availability

- All data reported in this paper will be shared by the lead contact upon request. This paper analyzes existing, publicly available data. These accession numbers for the datasets are listed in the key resources table.
- This paper does not report original code.
- Any additional information required to reanalyze the data reported in this paper is available from the lead contact upon request.

EXPERIMENTAL MODEL AND STUDY PARTICIPANT DETAILS

Drosophila melanogaster strains were reared on a standard cornmeal/agar medium supplemented with yeast under 12:12LD cycles at 25°C. Heterozygous genetic controls used in behavioral experiments were parental strains crossed to w1118 wild-type flies. Young flies (3-7 days) were used in all experiments. Every experiment was repeated at least twice. Strains used in this study are listed in the Key Resources Table.

METHOD DETAILS

Immunohistochemistry

Whole flies were fixed in PBS with 4% paraformaldehyde and 0.5% Triton X-100 for 2.5 hours while rotating at room temperature. Flies were then washed in PBS with 0.5% Triton X-100 (PBST) for 3x 10 minutes before brains were removed via dissection. Dissected brains were washed 3x 15 minutes and blocked with 10% normal goat serum (NGS; Jackson Labs) in 0.5% PBST (blocking buffer) for 2 hours at room temperature or overnight at 4°C. Brains were then incubated at 4°C overnight in blocking buffer with the following antibodies and concentrations: chicken anti-GFP (1:1000; Abcam ab13970), rabbit anti-per (1:1000; Rosbash Lab), and rabbit anti-dsRed (Takara Bio 632393; 1:200). Then, brains were incubated with secondary antibodies (Alexa Fluor 488-conjugated anti-chicken, AlexA Fluor 633-conjugated anti-rabbit) diluted at 1:500 in blocking buffer for two hours at room temperature, and washed 3x 15 minutes with 0.5% PBST. Stained brains were mounted in VectaShield mounting medium (Vector Laboratories, Newark, CA). Images were acquired using a Leica Stellaris 8 confocal microscope or a Leica SP5 confocal microscope equipped with a white-light laser and a 40X oil objective, and processing was done using Fiji.[56]

Optogenetic Locomotor Behavior

Optogenetic experiments were done in FlyBoxes, as previously described.[38] Flies were aged 2-5 days old and loaded into individual wells of white 96-well plates containing 300uL of food with 5% sucrose, 2% agar, and 400uM all trans-retinal (Sigma Aldrich, R2500). Within a FlyBox, the plate is illuminated from underneath with infrared light supplied by an 850 nm LED board (LUXEON). Images of loaded plates were captured every ten seconds using a down-facing USB webcam (Logistic C910 with infrared light filter removed) placed at the top of the box and with Image Capture software. Entrainment light with a 12:12 LD cycle was provided by a white LED strip set to the minimum brightness at ~10 lux. Optogenetic stimulation was given using high power red (~0.9 uW/mm^2 at 625 nm) or green (~6 uW/mm^2 at 525 nm) LEDs pulsing at 5 Hz. All lights were controlled with an Arduino in the FlyBox. Each experiment included two full entrainment days and one baseline day before optogenetic manipulation. All experiments were conducted at ambient room temperature.

Standard Locomotor Behavior

Standard experiments were done using the Drosophila Activity Monitor (DAM) system (Trikinetics, Waltham, MA), as previously described.[57] Flies were aged 2-5 days old and loaded into individual glass tubes with 5% sucrose and 2% agar food on one end and a stopper on the other. Glass tubes with flies were then loaded onto DAMs, which recorded the number of beam crosses a fly makes. All experiments were conducted with 12:12 LD in 25°C incubators. Flies were entrained for two full days, and activity and sleep were averaged across the 2-3 days thereafter.

Single-Cell RNA Sequencing

Single-cell RNA sequencing experiments and analyses were done by and reported in Ma et al., 2021. Briefly, flies expressing a fluorescent protein under the control of *Clk856-GAL4* were entrained and dissected at timepoints every four hours around the clock. Brains were dissociated into a single-cell suspension and sorted using a fluorescence-activated cell sorting (FACS) machine (BD Biosciences, Franklin Lakes, New Jersey). Single-cell RNA library preparation was done using a modified version of CEL-Seq2.[58,59]

Ex Vivo EPAC Functional Live Imaging

UAS-EPAC-H187 or 10XUAS-cAMPFIRE-M were expressed in ITP$^+$ LNs using *ss00639-GAL4*. Flies aged 0-5 days old were collected and entrained in 12:12 LD for at least two full days. Flies were collected in the light phase between ZT01 and ZT03 or in the dark phase between ZT13 and ZT15 for testing. Adult female brains were dissected in adult hemolymph-like saline (AHL; 108 mM NaCl, 5mM KCl, 2 mM $CaCl_2$, 8.2 mM $MgCl_2$, 4 mM $NaHCO_3$, 1 mM NaH_2PO_4, 5 mM trehalose, 10 mM sucrose, 5 mM HEPES; pH 7.5) (Cold Spring Harbor Protocols, 2013) and 1 uM tetrodotoxin (AHL-TTX). Brains were mounted onto a poly-l-lysine-coated cover slip (Neuvitro Corporation, Camas, WA) on a SYLGARD 184-coated perfusion chamber (Automate Scientific, Berkeley, CA) with a bath of AHL-TTX. Perfusion flow was established at 2 drops per second with a gravity-fed ValveBank II perfusion system (Automate Scientific, Berkeley, CA), and waste was

collected with a vacuum pump. Recording was started after the brains had been in AHL-TTX for at least five minutes.

Images were acquired on a Leica Stellaris 8 with confocal imaging equipped with a white-light laser and 405 nm diode. Using LAS X software (Leica, Wetzlar, Germany), we recorded XYZT in Live Imaging Mode. Using a 20X water objective with 0.5 numerical aperture (Leica, Wetzlar, Germany), images were acquired at 512x512 with the pinhole setting at 6.73. CFP was excited with a 440 nm laser and detected using an HyD S2 sensor, while YFP was detected using an HyD S 4 sensor. Laser intensities and detector gains were kept consistent within individual experiments. With both the ITP^{+} LNd and the 5^{th} s-LNv in frame, z-positions were set for both cells. Images of both z-positions were taken every two seconds. Recordings included one minute of baseline recording with AHL-TTX.

QUANTIFICATION AND STATISTICAL ANALYSIS

Statistical analyses were performed using R-based web application Statistics Kingdom (https://www.statskingdom.com). Details of tests can be found in figure legends.

EM Connectome Analysis

Hemibrain EM connectome data[21] was accessed and analyzed with NeuPrint.[30] To identify our neurons of interest, we used the “Find Neurons” function and recorded their BodyIDs. To compare morphologies, we entered BodyIDs into the “Skeleton” visualization function. To look at connectivity strengths, we entered BodyIDs into the “Connectivity Graph” function. Whole brain EM connectome data[24] was accessed and analyzed with FlyWire.[23] To identify our neurons of interest, we used the “Search Cells and Annotations” function and recorded their IDs. To look at connectivity, we entered IDs into the “Network” function. Boxplots were created using R-based web application BoxplotR (http://shiny.chemgrid.org/boxplotr/).

Behavior Analysis

Fly locomotor activity was extracted from the images using pySolo[61] and pre-processed with DAMFileScan (Trikinetics, Waltham, MA) in optogenetic locomotor behavior assays. Data was pre-processed with DAMFileScan (Trikinetics, Waltham, MA) in standard locomotor behavior assays. Activity and sleep data from both optogenetic and standard locomotor behavior experiments were analyzed with the Sleep and Circadian Analysis MATLAB Program (SCAMP, Vecsey Lab).[62] P-wake and p-doze analyses were done using the Fly Sleep Probability analysis package.[40] Error bars and shaded regions in the time series plots are 95% confidence intervals of the means. For all box plots, center lines indicate medians, box limits indicate 25^{th} and 75^{th} percentiles, and whiskers extend 1.5 times the interquartile range. All plots were created in Python using the seaborn package.

Single-Cell Sequencing Analysis

Original data and primary analysis was done by Ma et al., 2021.[16] Transcripts per 10 thousand (TP10K) data from this previous paper was used in the current study. tSNE plots

were created in R using the Seurat package.[63] Timeseries plot was created in Python using the seaborn package.

Ex Vivo EPAC Functional Live Imaging Analysis

Images were analyzed with custom MATLAB code modified from Adel et al., 2022. CFP and YFP signals were individually extracted using hand-drawn ROIs, and they were normalized to background signal. The ratio CFP/YFP indicates cAMP signal. Then, ΔF/F was calculated, with the average of 10 seconds before the onset of dopamine perfusion acting as a baseline. Python was used to plot the time series with a simple moving average of two data points and with the shaded regions signifying the 68% confidence interval of the mean. All plots were created in Python using the seaborn package.

Supplementary Material

Refer to Web version on PubMed Central for supplementary material.

Acknowledgements

Many thanks to members of the Rosbash Lab for helpful discussions and help with this work, especially, Dr. Shlesha Richhariya and Dr. Kate Abruzzi. We thank our former colleague Dr. Fang Guo for establishing optogenetic experiments in the lab. Thank you very much also to Mohamed Adel from the Griffith Lab at Brandeis University particularly for help with imaging analysis and former member Dr. Timothy Wiggin for a lot of initial help with behavior analysis.

Thank you to Dr. Heather Dionne, Dr. Aljoscha Nern, Dr. Gerry Rubin from Janelia Research Campus for generously sharing unpublished fly lines. We also thank the Yi Rao lab for sharing Chemoconnectome lines with us and Dr. Bing Ye, Dr. Elizabeth Cebul, and Dr. Haining Zhong lab for developing and sharing unpublished cAMPFIRE constructs with us.

We thank the Princeton FlyWire team and members of the Murthy and Seung labs, as well as members of the Allen Institute for Brain Science, for development and maintenance of FlyWire (supported by BRAIN Initiative grants MH117815 and NS126935 to Murthy and Seung). We also acknowledge members of the Princeton FlyWire team and the FlyWire consortium for neuron proofreading and annotation.

This work was supported by the Howard Hughes Medical Institute, the National Institute of Mental Health Neuroscience Training Grant (NIH grant no. MH019929), and the National Institute of General Medical Sciences Genetics Training Grant (NIH grant no. GM007122).

References

1. Borbély AA (1982). Two Process Model. Hum. Neurobiol 1, 195–204. [PubMed: 7185792]
2. Blume C, Garbazza C, and Spitschan M (2019). Effects of light on human circadian rhythms, sleep and mood. Somnologie 23, 147. 10.1007/S11818-019-00215-X. [PubMed: 31534436]
3. Tassi P, and Muzet A (2000). Sleep inertia. Sleep Med. Rev 4, 341–353. 10.1053/SMRV.2000.0098. [PubMed: 12531174]
4. Gabel V, Maire M, Reichert CF, Chellappa SL, Schmidt C, Hommes V, Viola AU, and Cajochen C (2013). Effects of Artificial Dawn and Morning Blue Light on Daytime Cognitive Performance, Well-being, Cortisol and Melatonin Levels. Chronobiol. Int 30, 988–997. 10.3109/07420528.2013.793196. [PubMed: 23841684]
5. Werken M. Van De, GimÉnez MC, Vries B. De, Beersma DGM, Van Someren EJW, and Gordijn MCM (2010). Effects of artificial dawn on sleep inertia, skin temperature, and the awakening cortisol response. J. Sleep Res 19, 425—435. 10.1111/J.1365-2869.2010.00828.X. [PubMed: 20408928]

6. Grima B, Chélot E, Xia R, and Rouyer F (2004). Morning and evening peaks of activity rely on different clock neurons of the Drosophila brain. Nature 431, 869–873. 10.1038/NATURE02935. [PubMed: 15483616]
7. Stoleru D, Peng Y, Agosto J, and Rosbash M (2004). Coupled oscillators control morning and evening locomotor behaviour of Drosophila. Nat. 2004 4317010 431, 862–868. 10.1038/nature02926.
8. Muraro NI, and Ceriani MF (2015). Acetylcholine from Visual Circuits Modulates the Activity of Arousal Neurons in Drosophila. J. Neurosci 35, 16315–16327. 10.1523/JNEUROSCI.1571-15.2015. [PubMed: 26674859]
9. Renn SCP, Park JH, Rosbash M, Hall JC, and Taghert PH (1999). A pdf neuropeptide gene mutation and ablation of PDF neurons each cause severe abnormalities of behavioral circadian rhythms in Drosophila. Cell 99, 791–802. 10.1016/S0092-8674(00)81676-1. [PubMed: 10619432]
10. Im SH, Li W, and Taghert PH (2011). PDFR and CRY Signaling Converge in a Subset of Clock Neurons to Modulate the Amplitude and Phase of Circadian Behavior in Drosophila. PLoS One 6. 10.1371/JOURNAL.PONE.0018974.
11. Rieger D, Shafer OT, Tomioka K, and Helfrich-Förster C (2006). Functional analysis of circadian pacemaker neurons in Drosophila melanogaster. J. Neurosci 26, 2531–2543. 10.1523/JNEUROSCI.1234-05.2006. [PubMed: 16510731]
12. Rieger D, Wülbeck C, Rouyer F, and Helfrich-Förster C (2009). Period gene expression in four neurons is sufficient for rhythmic activity of Drosophila melanogaster under dim light conditions. J. Biol. Rhythms 24, 271–282. 10.1177/0748730409338508. [PubMed: 19625729]
13. Im SH, and Taghert PH (2010). PDF receptor expression reveals direct interactions between circadian oscillators in Drosophila. J. Comp. Neurol 518, 1925–1945. 10.1002/CNE.22311. [PubMed: 20394051]
14. Yoshii T, Hermann-Luibl C, Kistenpfennig C, Schmid B, Tomioka K, and Helfrich-Förster C (2015). Cryptochrome-Dependent and -Independent Circadian Entrainment Circuits in Drosophila. J. Neurosci 35, 6131. 10.1523/JNEUROSCI.0070-15.2015. [PubMed: 25878285]
15. Yao Z, and Shafer OT (2014). The Drosophila circadian clock is a variably coupled network of multiple peptidergic units. Science (80-.). 343, 1516–1520. 10.1126/science.1251285.
16. Ma D, Przybylski D, Abruzzi KC, Schlichting M, Li Q, Long X, and Rosbash M (2021). A transcriptomic taxonomy of drosophila circadian neurons around the clock. Elife 10, 1–19. 10.7554/eLife.63056.
17. Lee G, Bahn JH, and Park JH (2006). Sex- and clock-controlled expression of the neuropeptide F gene in Drosophila. Proc. Natl. Acad. Sci. U. S. A 103, 12580–12585. 10.1073/PNAS.0601171103. [PubMed: 16894172]
18. Hermann C, Yoshii T, Dusik V, and Helfrich-Förster C (2012). Neuropeptide F immunoreactive clock neurons modify evening locomotor activity and free-running period in Drosophila melanogaster. J. Comp. Neurol 520, 970–987. 10.1002/CNE.22742. [PubMed: 21826659]
19. Johard HAD, Yoishii T, Dircksen H, Cusumano P, Rouyer F, Helfrich-Förster C, and Nässel DR (2009). Peptidergic clock neurons in Drosophila: Ion transport peptide and short neuropeptide F in subsets of dorsal and ventral lateral neurons. J. Comp. Neurol 516, 59–73. 10.1002/CNE.22099. [PubMed: 19565664]
20. Hermann-Luibl C, Yoshii T, Senthilan PR, Dircksen H, and Helfrich-Förster C (2014). The ion transport peptide is a new functional clock neuropeptide in the fruit fly drosophila melanogaster. J. Neurosci 34, 9522–9536. 10.1523/JNEUROSCI.0111-14.2014. [PubMed: 25031396]
21. Scheffer LK, Xu CS, Januszewski M, Lu Z, Takemura SYSSYS, Hayworth KJ, Huang GB, Shinomiya K, Maitin-Shepard J, Berg S, et al. (2020). A connectome and analysis of the adult drosophila central brain. Elife 9, 1–74. 10.7554/ELIFE.57443.
22. Shafer OT, Gutierrez GJ, Li K, Mildenhall A, Spira D, Marty J, Lazar AA, and Fernandez MP (2022). Connectomic Analysis of the Drosophila Lateral Neuron Clock Cells Reveals the Synaptic Basis of Functional Pacemaker Classes. Elife 11.
23. Dorkenwald S, Matsliah A, Sterling AR, Schlegel P, Yu S-C, McKellar CE, Lin A, Costa M, Eichler K, Yin Y, et al. (2023). Neuronal wiring diagram of an adult brain. bioRxiv Prepr. Serv. Biol 10.1101/2023.06.27.546656.

24. Schlegel P, Yin Y, Bates AS, Dorkenwald S, Eichler K, Brooks P, Han DS, Gkantia M, Dos Santos M, Munnelly EJ, et al. (2023). Whole-brain annotation and multi-connectome cell typing quantifies circuit stereotypy in Drosophila. bioRxiv Prepr. Serv. Biol 10.1101/2023.06.27.546055.
25. Abruzzi KC, Zadina A, Luo W, Wiyanto E, Rahman R, Guo F, Shafer O, and Rosbash M (2017). RNA-seq analysis of Drosophila clock and non-clock neurons reveals neuron-specific cycling and novel candidate neuropeptides. PLOS Genet. 13, e1006613. 10.1371/journal.pgen.1006613. [PubMed: 28182648]
26. Ma D, Herndon N, Le JQ, Abruzzi KC, Zinn K, and Rosbash M (2023). Neural connectivity molecules best identify the heterogeneous clock and dopaminergic cell types in the Drosophila adult brain. Sci. Adv 9. 10.1126/SCIADV.ADE8500/SUPPL_FILE/SCIADV.ADE8500_TABLE_S2.ZIP.
27. Shang Y, Haynes P, Pírez N, Harrington KI, Guo F, Pollack J, Hong P, Griffith LC, and Rosbash M (2011). Imaging analysis of clock neurons reveals light buffers the wake-promoting effect of dopamine. Nat. Neurosci 14, 889–895. 10.1038/nn.2860. [PubMed: 21685918]
28. Fernandez-Chiappe F, Hermann-Luibl C, Peteranderl A, Reinhard N, Senthilan PR, Hieke M, Selcho M, Yoshii T, Shafer OT, Muraro NI, et al. (2020). Dopamine signaling in wake-promoting clock neurons is not required for the normal regulation of sleep in drosophila. J. Neurosci 40, 9617–9633. 10.1523/JNEUROSCI.1488-20.2020. [PubMed: 33172977]
29. Schlichting M, Richhariya S, Herndon N, Ma D, Xin J, Lenh W, Abruzzi K, and Rosbash M (2022). Dopamine and GPCR-mediated modulation of DN1 clock neurons gates the circadian timing of sleep. Proc. Natl. Acad. Sci 119. 10.1073/pnas.2206066119.
30. Plaza SM, Clements J, Dolafi T, Umayam L, Neubarth NN, Scheffer LK, and Berg S (2022). neuPrint: An open access tool for EM connectomics. Front. Neuroinform 16, 73. 10.3389/FNINF.2022.896292/BIBTEX.
31. Gummadova JO, Coutts GA, and Glossop NRJ (2009). Analysis of the Drosophila Clock Promoter Reveals Heterogeneity in Expression between Subgroups of Central Oscillator Cells and Identifies a Novel Enhancer Region. 10.1177/0748730409343890 24, 353–367. 10.1177/0748730409343890.
32. Deng B, Li Q, Liu X, Cao Y, Li B, Qian Y, Xu R, Mao R, Zhou E, Zhang W, et al. (2019). Chemoconnectomics: Mapping Chemical Transmission in Drosophila. Neuron 101, 876–893.e4. [PubMed: 30799021]
33. Helfrich-Förster C, Edwards T, Yasuyama K, Wisotzki B, Schneuwly S, Stanewsky R, Meinertzhagen IA, and Hofbauer A (2002). The Extraretinal Eyelet of Drosophila: Development, Ultrastructure, and Putative Circadian Function. J. Neurosci 22, 9255–9266. 10.1523/JNEUROSCI.22-21-09255.2002. [PubMed: 12417651]
34. Malpel S, Klarsfeld A, and Rouyer F (2002). Larval optic nerve and adult extra-retinal photoreceptors sequentially associate with clock neurons during Drosophila brain development. Development 129, 1443–1453. 10.1242/DEV.129.6.1443. [PubMed: 11880353]
35. Schubert FK, Hagedorn N, Yoshii T, Helfrich-Förster C, and Rieger D (2018). Neuroanatomical details of the lateral neurons of *Drosophila melanogaster* support their functional role in the circadian system. J. Comp. Neurol 526, 1209–1231. 10.1002/cne.24406. [PubMed: 29424420]
36. Li M-T, Cao L-H, Xiao N, Tang M, Deng B, Yang T, Yoshii T, and Luo D-G (2018). Hub-organized parallel circuits of central circadian pacemaker neurons for visual photoentrainment in Drosophila. Nat. Commun 9, 4247. 10.1038/S41467-018-06506-5. [PubMed: 30315165]
37. Richhariya S, Shin D, Le JQ, and Rosbash M (2023). Dissecting neuron-specific functions of circadian genes using modified cell-specific CRISPR approaches. Proc. Natl. Acad. Sci. U. S. A 120, e2303779120. 10.1073/PNAS.2303779120/SUPPL_FILE/PNAS.2303779120.SD01.XLSX. [PubMed: 37428902]
38. Guo F, Chen X, and Rosbash M (2017). Temporal calcium profiling of specific circadian neurons in freely moving flies. Proc. Natl. Acad. Sci 114, E8780–E8787. 10.1073/pnas.1706608114. [PubMed: 28973886]
39. Klapoetke NC, Murata Y, Kim SS, Pulver SR, Birdsey-Benson A, Cho YK, Morimoto TK, Chuong AS, Carpenter EJ, Tian Z, et al. (2014). Independent optical excitation of distinct neural populations. Nat. Methods 2014 113 11, 338–346. 10.1038/nmeth.2836.

40. Wiggin TD, Goodwin PR, Donelson NC, Liu C, Trinh K, Sanyal S, and Griffith LC (2020). Covert sleep-related biological processes are revealed by probabilistic analysis in *Drosophila*. Proc. Natl. Acad. Sci 117, 10024–10034. 10.1073/pnas.1917573117. [PubMed: 32303656]
41. Wu M, Nern A, Williamson WR, Morimoto MM, Reiser MB, Card GM, and Rubin GM (2016). Visual projection neurons in the Drosophila lobula link feature detection to distinct behavioral programs. Elife 5. 10.7554/eLife.21022.
42. Johns DC, Marx R, Mains RE, O'Rourke B, and Marbán E (1999). Inducible Genetic Suppression of Neuronal Excitability. J. Neurosci 19, 1691–1697. 10.1523/JNEUROSCI.19-05-01691.1999. [PubMed: 10024355]
43. Thum AS, Knapek S, Rister J, Dierichs-Schmitt E, Heisenberg M, and Tanimoto H (2006). Differential potencies of effector genes in adult Drosophila. J. Comp. Neurol 498, 194–203. 10.1002/CNE.21022. [PubMed: 16856137]
44. Guo F, Cerullo I, Chen X, and Rosbash M (2014). PDF neuron firing phase-shifts key circadian activity neurons in Drosophila. Elife 2014. 10.7554/ELIFE.02780.
45. Liu Q, Liu S, Kodama L, Driscoll MR, and Wu MN (2012). Two dopaminergic neurons signal to the dorsal fan-shaped body to promote wakefulness in Drosophila. Curr. Biol 22, 2114–2123. 10.1016/j.cub.2012.09.008. [PubMed: 23022067]
46. Schlichting M, Díaz MM, Xin J, and Rosbash M (2019). Neuron-specific knockouts indicate the importance of network communication to drosophila rhythmicity. Elife 8. 10.7554/eLife.48301.
47. Karam CS, Jones SK, and Javitch JA (2020). Come Fly with Me: An overview of dopamine receptors in Drosophila melanogaster. Basic Clin. Pharmacol. Toxicol 126 Suppl 6, 56–65. 10.1111/BCPT.13277. [PubMed: 31219669]
48. Klarenbeek J, Goedhart J, Van Batenburg A, Groenewald D, and Jalink K (2015). Fourth-Generation Epac-Based FRET Sensors for cAMP Feature Exceptional Brightness, Photostability and Dynamic Range: Characterization of Dedicated Sensors for FLIM, for Ratiometry and with High Affinity. PLoS One 10, e0122513. 10.1371/JOURNAL.PONE.0122513. [PubMed: 25875503]
49. Pfeiffer BD, Ngo T-TB, Hibbard KL, Murphy C, Jenett A, Truman JW, and Rubin GM (2010). Refinement of Tools for Targeted Gene Expression in Drosophila. Genetics 186, 735–755. 10.1534/genetics.110.119917. [PubMed: 20697123]
50. Massengill CI, Bayless-Edwards L, Ceballos CC, Cebul ER, Cahill J, Bharadwaj A, Wilson E, Qin M, Whorton MR, Baconguis I, et al. (2022). Sensitive genetically encoded sensors for population and subcellular imaging of cAMP in vivo. Nat. Methods 2022 1911 19, 1461–1471. 10.1038/s41592-022-01646-5.
51. Liang X, Holy TE, and Taghert PH (2017). A Series of Suppressive Signals within the Drosophila Circadian Neural Circuit Generates Sequential Daily Outputs. Neuron 94, 1173–1189.e4. 10.1016/J.NEURON.2017.05.007. [PubMed: 28552314]
52. Liang X, Holy TE, and Taghert PH (2016). Synchronous *Drosophila* circadian pacemakers display nonsynchronous Ca^{2+} rhythms in vivo. Science (80-.). 351, 976–981. 10.1126/science.aad3997.
53. Xie T, Ho MCW, Liu Q, Horiuchi W, Lin CC, Task D, Luan H, White BH, Potter CJ, and Wu MN (2018). A Genetic Toolkit for Dissecting Dopamine Circuit Function in Drosophila. Cell Rep. 23, 652–665. 10.1016/J.CELREP.2018.03.068. [PubMed: 29642019]
54. Schlichting M, Weidner P, Diaz M, Menegazzi P, Dalla Benetta E, Helfrich-Förster C, and Rosbash M (2019). Light-Mediated Circuit Switching in the Drosophila Neuronal Clock Network. Curr. Biol 29, 3266–3276.e3. 10.1016/j.cub.2019.08.033. [PubMed: 31564496]
55. Duhart JM, Herrero A, de la Cruz G, Ispizua JI, Pírez N, and Ceriani MF (2020). Circadian Structural Plasticity Drives Remodeling of E Cell Output. Curr. Biol 30, 5040–5048.e5. 10.1016/j.cub.2020.09.057. [PubMed: 33065014]
56. Schindelin J, Arganda-Carreras I, Frise E, Kaynig V, Longair M, Pietzsch T, Preibisch S, Rueden C, Saalfeld S, Schmid B, et al. (2012). Fiji: An open-source platform for biological-image analysis. Nat. Methods 9, 676–682. 10.1038/NMETH.2019. [PubMed: 22743772]
57. Pfeiffenberger C, Lear BC, Keegan KP, and Allada R (2010). Locomotor Activity Level Monitoring Using the *Drosophila* Activity Monitoring (DAM) System: Figure 1. Cold Spring Harb. Protoc 2010, pdb.prot5518. 10.1101/pdb.prot5518.

58. Paul A, Crow M, Raudales R, He M, Gillis J, and Huang ZJ (2017). Transcriptional Architecture of Synaptic Communication Delineates GABAergic Neuron Identity. Cell 171, 522–539.e20. 10.1016/j.cell.2017.08.032. [PubMed: 28942923]

59. Hashimshony T, Senderovich N, Avital G, Klochendler A, de Leeuw Y, Anavy L, Gennert D, Li S, Livak KJ, Rozenblatt-Rosen O, et al. (2016). CEL-Seq2: Sensitive highly-multiplexed single-cell RNA-Seq. Genome Biol. 17, 1–7. 10.1186/s13059-016-0938-8. [PubMed: 26753840]

60. Drosophila Adult Hemolymph-Like Saline (AHLS) (2013). Cold Spring Harb. Protoc 2013, pdb.rec079459. 10.1101/PDB.REC079459.

61. Gilestro GF, and Cirelli C (2009). pySolo: a complete suite for sleep analysis in Drosophila. Bioinformatics 25, 1466–1467. 10.1093/BIOINFORMATICS/BTP237. [PubMed: 19369499]

62. Vecsey CG, Koochagian C, Porter MT, Roman G, and Sitaraman D (2024). Analysis of Sleep and Circadian Rhythms from Drosophila Activity-Monitoring Data Using SCAMP. Cold Spring Harb. Protoc 10.1101/PDB.PROT108182.

63. Stuart T, Butler A, Hoffman P, Hafemeister C, Papalexi E, Mauck WM, Hao Y, Stoeckius M, Smibert P, and Satija R (2019). Comprehensive Integration of Single-Cell Data. Cell 177, 1888–1902.e21. 10.1016/J.CELL.2019.05.031/ATTACHMENT/2F8B9EBE-54E6-43EB-9EF2-949B6BDA8BA2/MMC3.PDF. [PubMed: 31178118]

64. Adel M, Chen N, Zhang Y, Reed ML, Quasney C, and Griffith LC (2022). Pairing-Dependent Plasticity in a Dissected Fly Brain Is Input-Specific and Requires Synaptic CaMKII Enrichment and Nighttime Sleep. J. Neurosci 42, 4297–4310. 10.1523/JNEUROSCI.0144-22.2022. [PubMed: 35474278]

Highlights

- ITP^+ LNs are wake-promoting circadian neurons.
- Dopamine 1-like receptor 1 (Dop1R1) mRNA is upregulated in ITP^+ LNs in the morning.
- Morning wakefulness is dependent on functional Dop1R1 expression in ITP^+ LNs.
- The morning cAMP response to dopamine in ITP^+ LNs is more rapid than the evening.

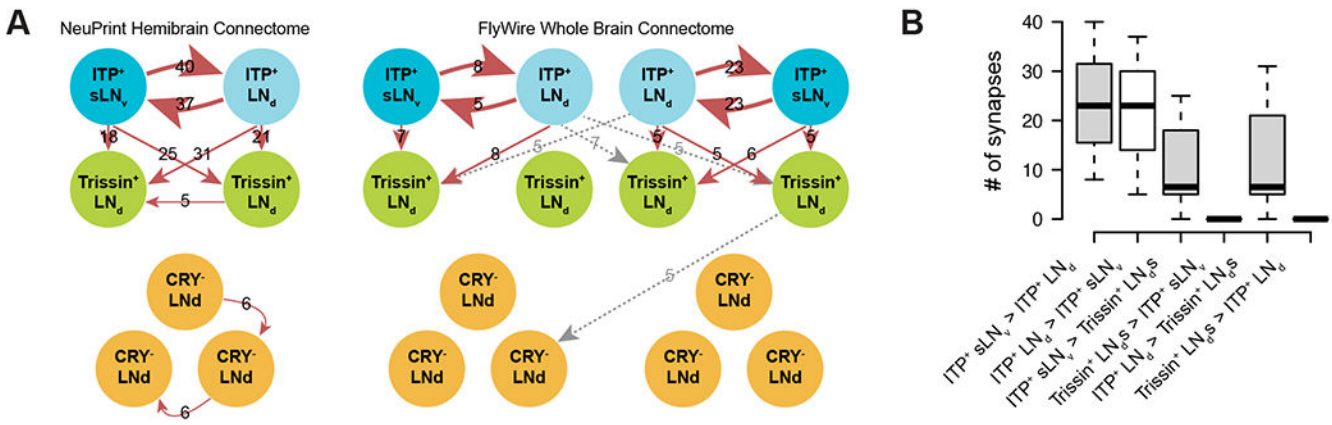

Figure 1. ITP-expressing lateral neurons top the evening cell connectomic hierarchy.

(A) EM connectivity graphs showing connectivity weights of the evening cells with a threshold of at least 5 synapses of the NeuPrint Hemibrain Connectome (left) [30] and the FlyWire Whole Brain Connectome (right) [23,24]. Direction of synapses are indicated by arrows and number of synapses are indicated by numbers. Gray dashed arrows indicate contralateral synapses.

(B) Boxplot quantifying number of synapses between ITP$^+$ sLN$_v$s, ITP$^+$ LN$_d$, and Trissin$^+$ LN$_d$s in individual directions from both the NeuPrint Hemibrain Connectome [30] and the FlyWire Whole Brain Connectome [23,24] datasets.

See also Figure S1.

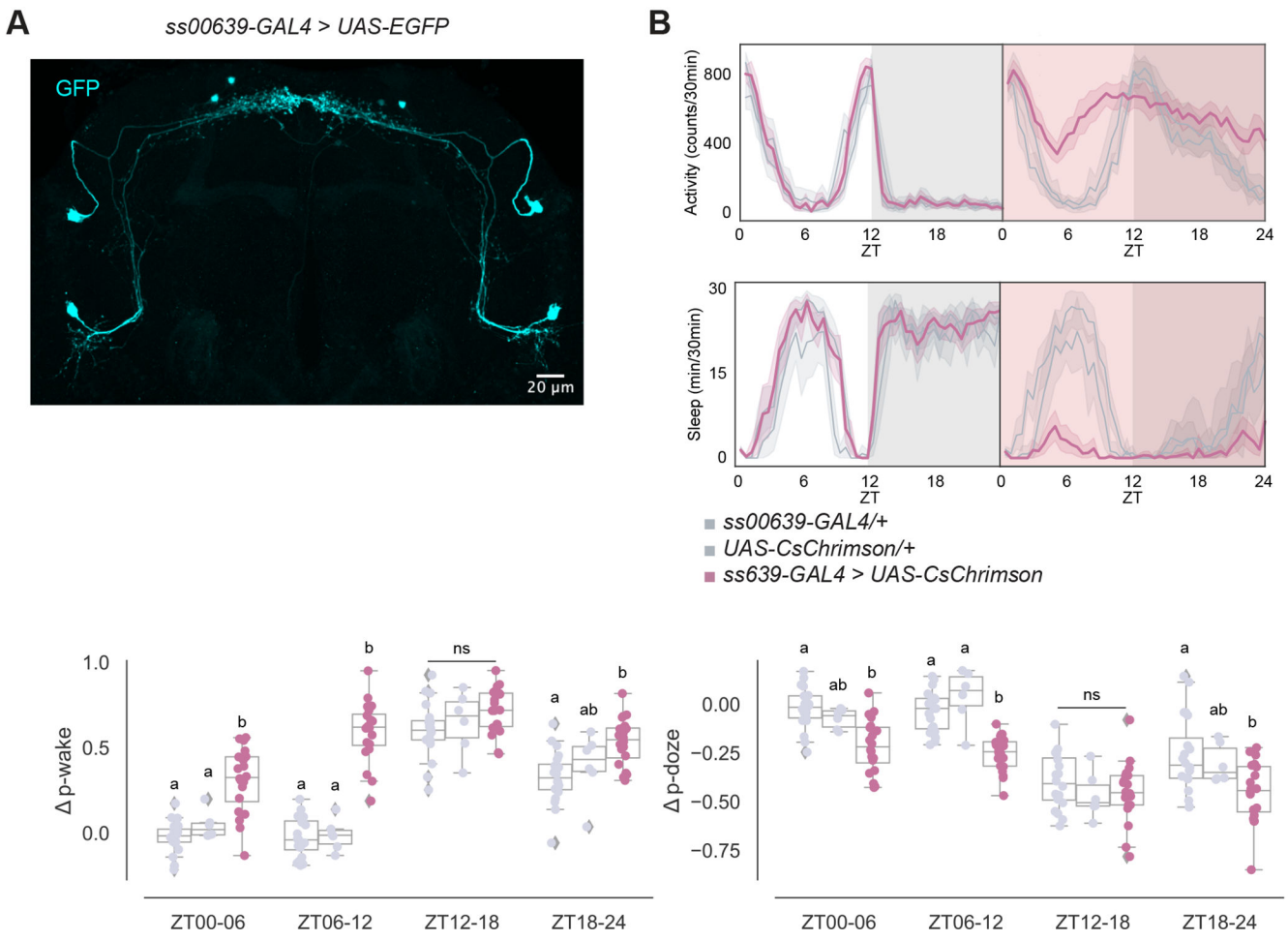

Figure 2. ITP$^+$ LNs are wake promoting circadian neurons.

(A) Representative whole-brain maximum intensity projection of *ss00639-GAL4* labeling ITP$^+$ LNs with GFP (cyan) antibody staining. Axonal bifurcations of the ITP$^+$ LN$_d$s are marked by white arrowheads.

(B) Timeseries plots of activity and sleep of female flies expressing red light-sensitive CsChrimson in ITP$^+$ LNs at baseline (left) and with 24-hour red LED optogenetic activation (right) in 12:12 LD. Heterozygous *ss00639-GAL4* (n=20) and *UAS-CsChrimson* (n=9) controls are in gray. Experimental flies (n=20) expressing both transgenes are colored. Bold lines are means and shaded regions are 95% confidence intervals of the means.

(C) Boxplots quantifying the change in p-wake (left) and p-doze (right) of female flies expressing red light-sensitive CsChrimson in ITP$^+$ LNs during the red LED optogenetic activation day from baseline day in six-hour time bins. Genotypes are depicted by the same color scheme as in (B). Letters represent statistically distinct groups as tested by a Kruskal Wallis test, post-hoc Mann Whitney U multiple comparisons method, and a Bonferroni-corrected significance value of $p < 0.01667$. Groups labeled with “ns” are not statistically distinct.

See also Figure S2.

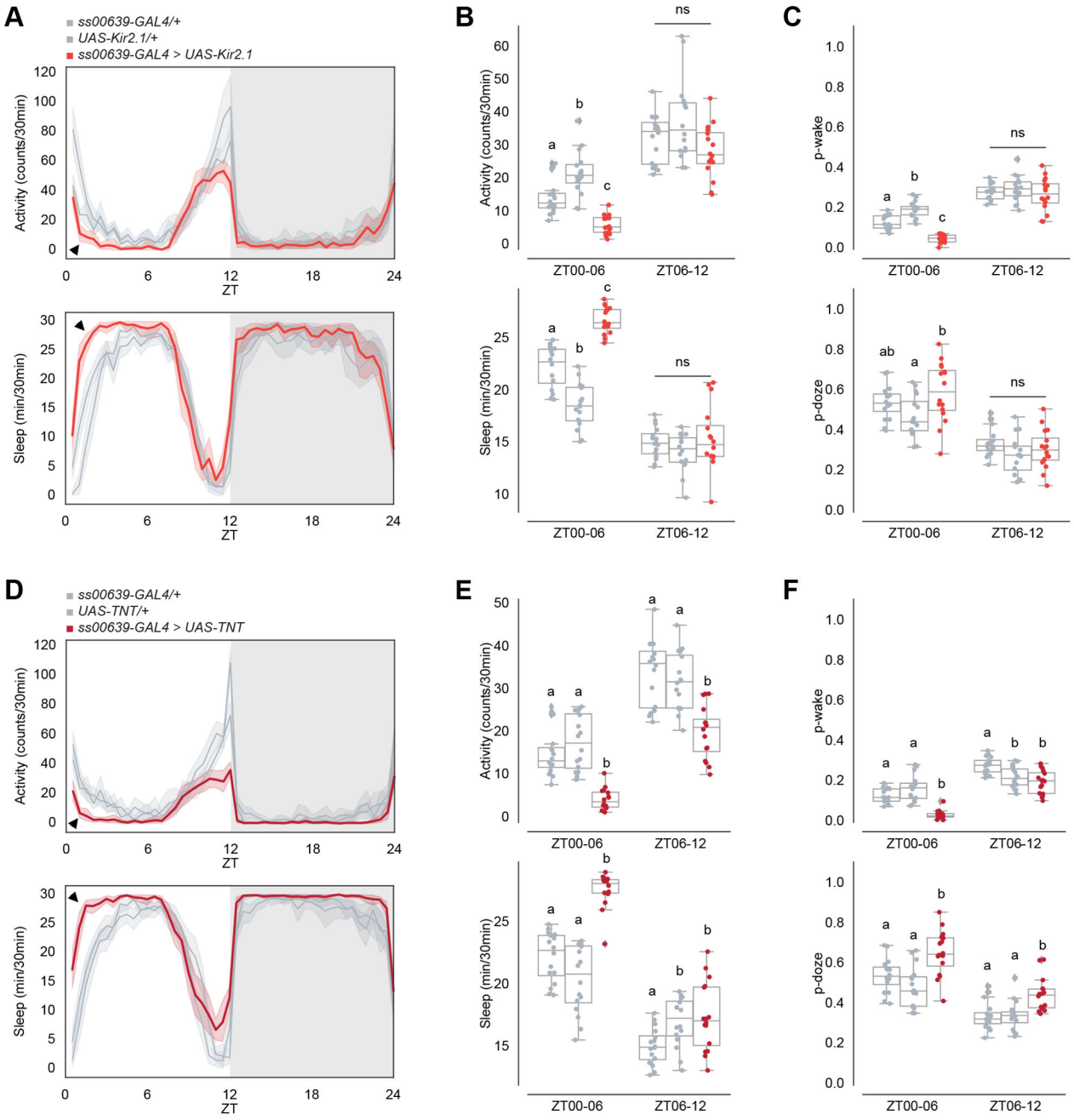

Figure 3. Inhibiting ITP^{+} LNs decreases morning wakefulness after the onset of light.

(A) Timeseries plots of activity (top) and sleep (bottom) of male flies expressing inhibitory Kir2.1 potassium channels in ITP^{+} LNs in 12:12 LD. Heterozygous *ss00639-GAL4* (n=16) and *UAS-Kir2.1* (n=16) controls are in gray. Experimental flies (n=16) expressing all transgenes are colored. Bold lines are means and shaded regions are 95% confidence intervals of the means. Black arrowheads point to the major difference between control and experimental flies between ZT00 and ZT06.

(B) Boxplots quantifying activity (top) and sleep (bottom) of male flies expressing inhibitory Kir2.1 potassium channels in ITP^+ LNs during ZT00-06 and ZT06-12 daytime bins. Genotypes are depicted by the same color scheme as in (A). Letters represent statistically distinct groups as tested by a Kruskal Wallis test, post-hoc Mann Whitney U multiple comparisons method, and a Bonferroni-corrected significance value of $p < 0.01667$. Groups labeled with “ns” are not statistically distinct.

(C) Boxplots quantifying p-wake (top) and p-doze (bottom) of male flies expressing inhibitory Kir2.1 potassium channels in ITP^+ LNs during ZT00-06 and ZT06-12 daytime bins. Genotypes are depicted by the same color scheme as in (A). Letters represent statistically distinct groups as tested by a Kruskal Wallis test, post-hoc Mann Whitney U multiple comparisons method, and a Bonferroni-corrected significance value of $p < 0.01667$. Groups labeled with “ns” are not statistically distinct.

(D) Timeseries plots of activity (top) and sleep (bottom) of male flies expressing synaptic transmission inhibitor TNT in ITP^+ LNs in 12:12 LD. Heterozygous *ss00639-GAL4* (n=16) and *UAS-TNT* (n=16) controls are in gray. Experimental flies (n=16) expressing all transgenes are colored. Bold lines are means and shaded regions are 95% confidence intervals of the means. Black arrowheads point to the major difference between control and experimental flies between ZT00 and ZT06.

(E) Boxplots quantifying activity (top) and sleep (bottom) of male flies expressing synaptic transmission inhibitor TNT in ITP^+ LNs during ZT00-06 and ZT06-12 daytime bins. Genotypes are depicted by the same color scheme as in (D). Letters represent statistically distinct groups as tested by a Kruskal Wallis test, post-hoc Mann Whitney U multiple comparisons method, and a Bonferroni-corrected significance value of $p < 0.01667$. Groups labeled with “ns” are not statistically distinct.

(F) Boxplots quantifying p-wake (top) and p-doze (bottom) of male flies expressing synaptic transmission inhibitor TNT in ITP^+ LNs during ZT00-06 and ZT06-12 daytime bins. Genotypes are depicted by the same color scheme as in (D). Letters represent statistically distinct groups as tested by a Kruskal Wallis test, post-hoc Mann Whitney U multiple comparisons method, and a Bonferroni-corrected significance value of $p < 0.01667$. Groups labeled with “ns” are not statistically distinct.

See also Figure S3.

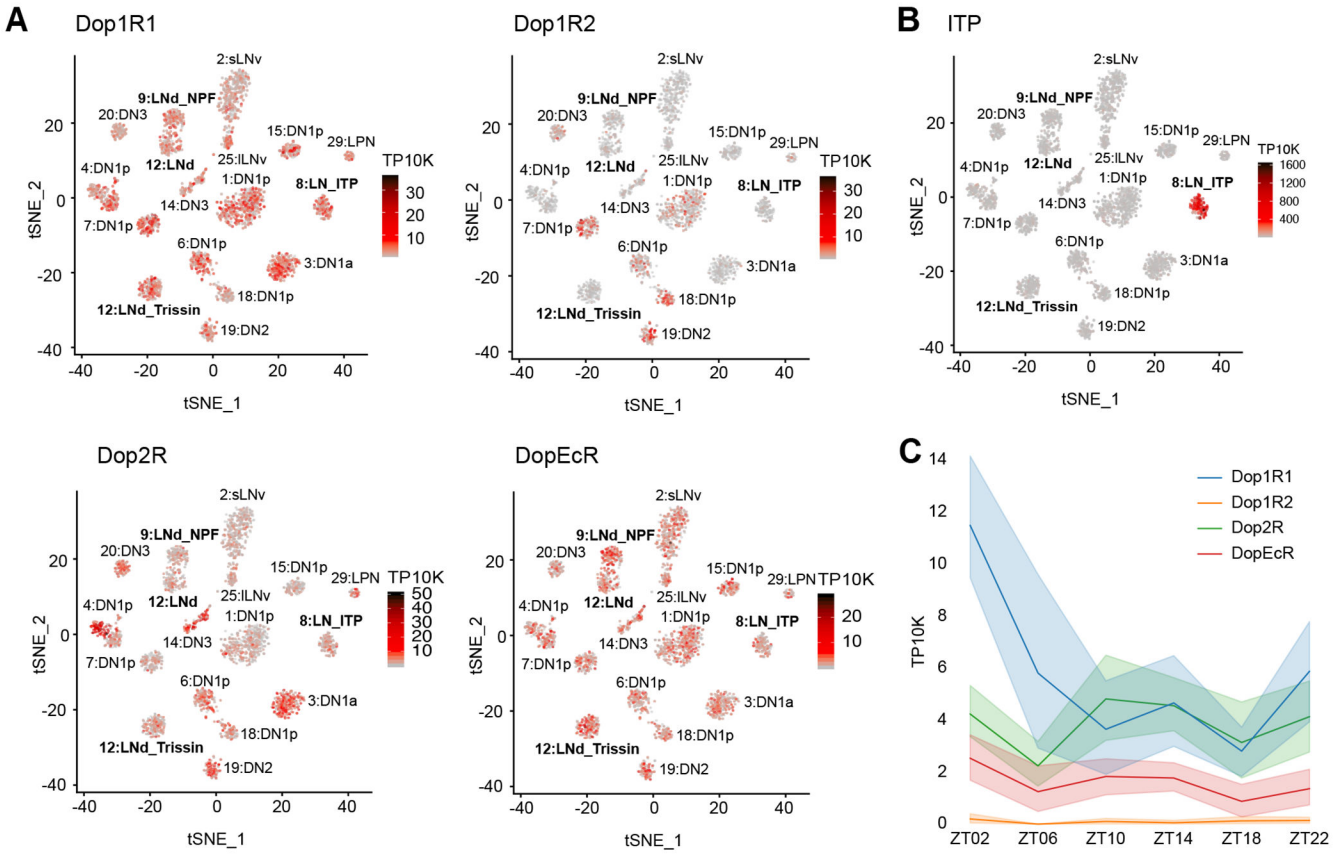

Figure 4. ITP^{+} LNs highly express *Dop1R1* mRNA.

(A) Single-cell RNA sequencing data of circadian neurons [4] displayed as tSNE plots and shaded by levels of dopamine receptor mRNA expression in number of transcripts per ten thousand transcripts. Each dot represents a single cell and each cluster represents a cell-type. Evening cell clusters marked by bold text.

(B) Single-cell RNA sequencing data of circadian neurons [4] displayed as a tSNE plot and shaded by levels of *ITP* mRNA expression in number of transcripts per ten thousand transcripts. Each dot represents a single cell and each cluster represents a cell-type. Evening cell clusters marked by bold text.

(C) Timeseries plot of dopamine receptor mRNA expression levels around the clock in ITP^{+} LNs in number of transcripts per ten thousand transcripts. Different colors represent different dopamine receptors mRNAs. Bold lines are means and shaded regions are 95% confidence intervals of the means.

See also Figure S4.

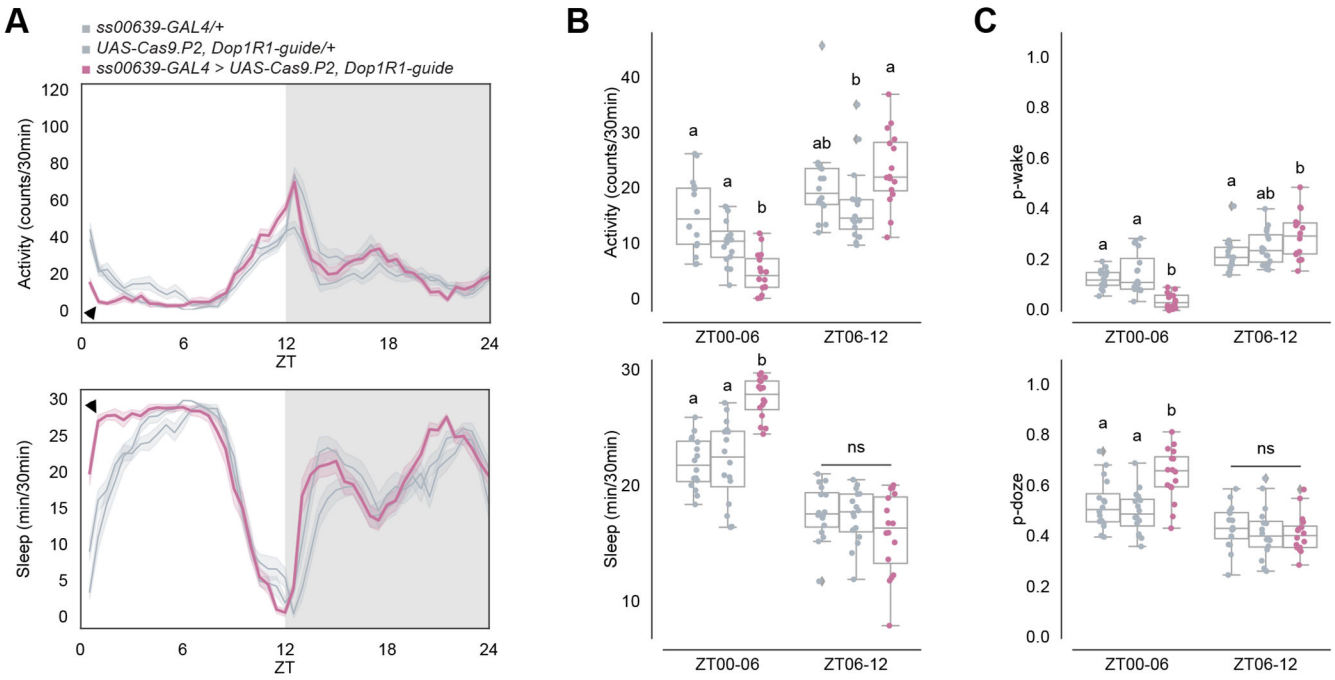

Figure 5. Functional knock-out of *Dop1R1* in ITP$^+$ LNs decreases morning wakefulness and increases sleep after the onset of light.

(A) Timeseries plots of activity (top) and sleep (bottom) of male flies with *Dop1R1* knock-out in ITP$^+$ LNs in 12:12 LD. Heterozygous *ss00639-GAL4* (n=16) and *UAS-Cas9.P2, Dop1R1-guide* (n=16) controls are in gray. Experimental flies (n=16) expressing all transgenes are colored. Bold lines are means and shaded regions are 95% confidence intervals of the means. Black arrowheads point to the major difference between control and experimental flies between ZT00 and ZT06.

(B) Boxplots quantifying activity (top) and sleep (bottom) of male flies with *Dop1R1* knock-out in ITP$^+$ LNs during ZT00-06 and ZT06-12 daytime bins. Genotypes are depicted by the same color scheme as in (A). Letters represent statistically distinct groups as tested by a Kruskal Wallis test, post-hoc Mann Whitney U multiple comparisons method, and a Bonferroni-corrected significance value of $p < 0.01667$. Groups labeled with “ns” are not statistically distinct.

(C) Boxplots quantifying p-wake (top) and p-doze (bottom) of male flies with *Dop1R1* knock-out in ITP$^+$ LNs during ZT00-06 and ZT06-12 daytime bins. Genotypes are depicted by the same color scheme as in (A). Letters represent statistically distinct groups as tested by a Kruskal Wallis test, post-hoc Mann Whitney U multiple comparisons method, and a Bonferroni-corrected significance value of $p < 0.01667$. Groups labeled with “ns” are not statistically distinct.

See also Figure S5.

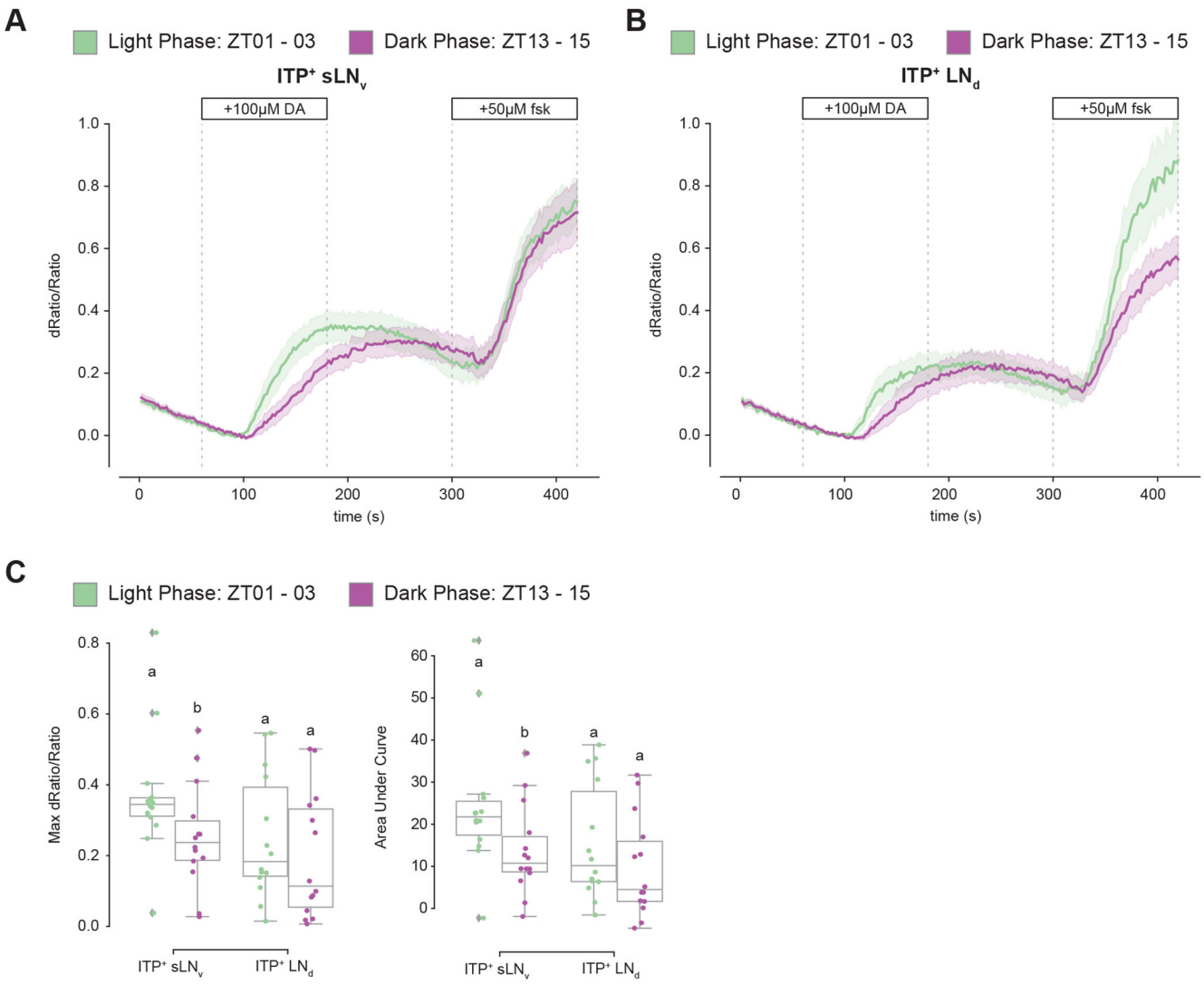

Figure 6. cAMP responses to dopamine are more robust during the day than the night.

(A) Timeseries plot of cAMP levels at baseline and in response to 100μM dopamine and 50μM forskolin perfusion as measured by *10XUAS-CAMPFIRE-M* in the ITP$^+$ sLN$_v$ during the light phase (green, n=14) and dark phase (purple, n=14). Bold lines are means shown with a simple moving average of two data points and shaded regions are 68% confidence intervals of the means. The linear section of the average light and dark phase responses have slopes of 4.50 x 10^{-3} and 3.16 x 10^{-3}, respectively.

(B) Timeseries plot of cAMP levels at baseline and in response to 100μM dopamine and 50μM forskolin perfusion as measured by *10XUAS-CAMPFIRE-M* in the ITP$^+$ LN$_d$ during the light phase (green, n=14) and dark phase (purple, n=14). Bold lines are means shown with a simple moving average of two data points and shaded regions are 68% confidence intervals of the means. The linear section of the average light and dark phase responses have slopes of 3.05 x 10^{-3} and 2.60 x 10^{-3}, respectively.

(C) Boxplots quantifying the maximum dRatio/Ratio (left, 100-180sec) and area under curve (right, 100-200sec) of the ITP$^+$ sLN$_v$ and ITP$^+$ LN$_d$ in response to 100μM dopamine

perfusion. Letters represent statistically distinct groups with p-value < 0.05 as tested by a Mann Whitney U test of individual cell-types.
See also Figure S6.

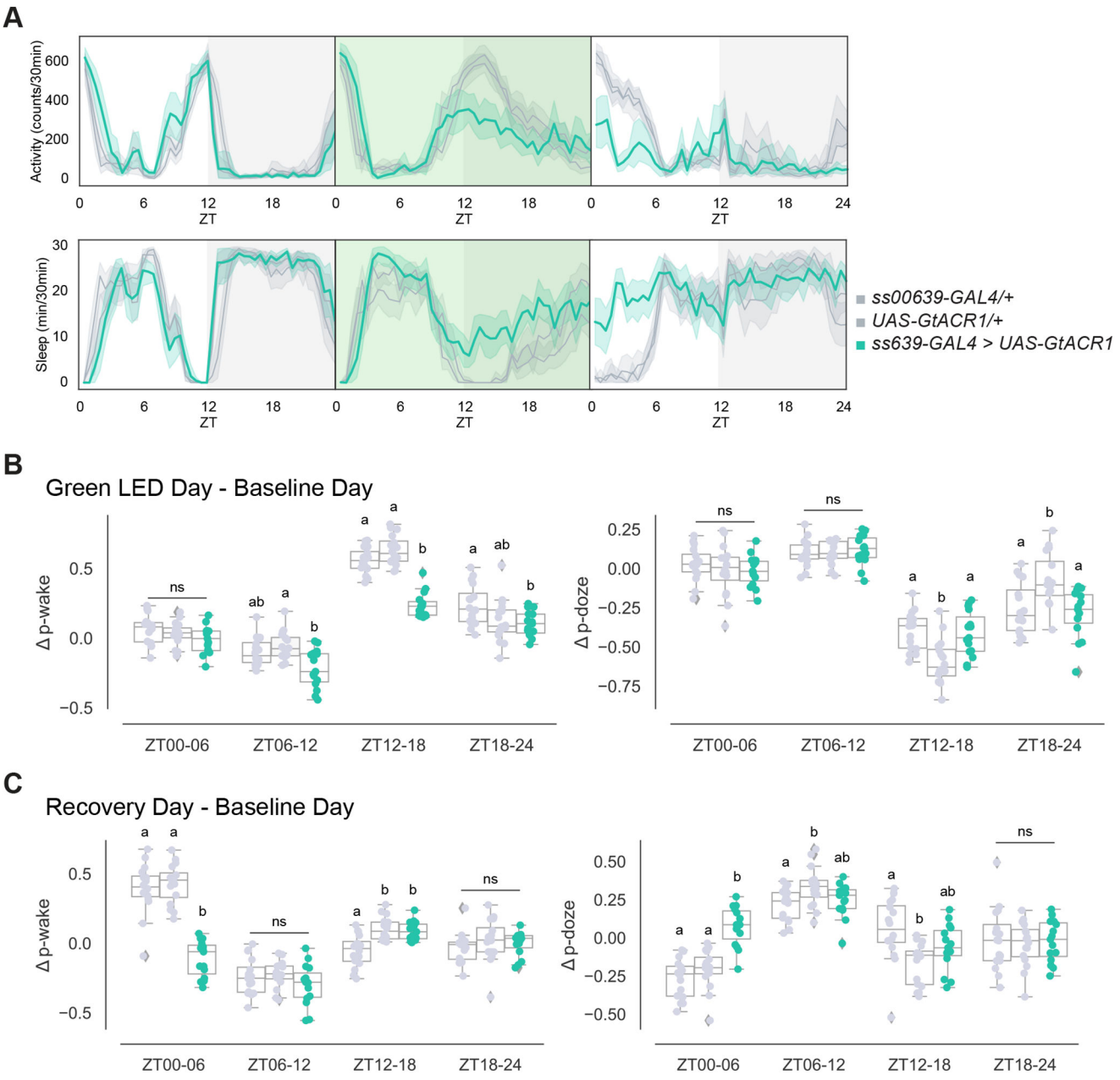

Figure 7. Acute inhibition of ITP$^+$ LNs leads to decreased morning wakefulness in the subsequent day

(A) Timeseries plots of activity and sleep of male flies expressing green light-sensitive GtACR1 in ITP$^+$ LNs at baseline (left), with 24-hour red LED optogenetic activation (middle), and during recovery (right) in 12:12 LD. Heterozygous *ss00639-GAL4* (n=16) and *UAS-GtACR1* (n=16) controls are in gray. Experimental flies (n=16) expressing both transgenes are colored. Bold lines are means and shaded regions are 95% confidence intervals of the means.

(B) Boxplots quantifying the change in p-wake (left) and p-doze (right) of male flies expressing green light-sensitive GtACR1 in ITP$^+$ LNs during the green LED optogenetic

activation day from baseline day in six-hour time bins. Genotypes are depicted by the same color scheme as in (A). Letters represent statistically distinct groups as tested by a Kruskal Wallis test, post-hoc Mann Whitney U multiple comparisons method, and a Bonferroni-corrected significance value of $p < 0.01667$. Groups labeled with “ns” are not statistically distinct.

(C) Boxplots quantifying the change in p-wake (left) and p-doze (right) of male flies expressing green light-sensitive GtACR1 in ITP^{+} LNs during the recovery day from baseline day in six-hour time bins. Genotypes are depicted by the same color scheme as in (A). Letters represent statistically distinct groups as tested by a Kruskal Wallis test, post-hoc Mann Whitney U multiple comparisons method, and a Bonferroni-corrected significance value of $p < 0.01667$. Groups labeled with “ns” are not statistically distinct.

Key resources table

REAGENT or RESOURCE	SOURCE	IDENTIFIER
Antibodies		
Chicken polyclonal anti-GFP	abcam	ab13970; RRID: AB_300798
Rabbit polyclonal anti-PER	Laboratory of Michael Rosbash	N/A
Goat anti-chicken IgY secondary antibody, Alexa Fluor 488	Thermo Fisher Scientific	A-11039; RRID: AB_142924
Goat anti-rabbit IgG cross-absorbed secondary antibody, Alexa Fluor 633	Thermo Fischer Scientfic	A-21070; RRID: AB_2535731
Chemicals, peptides, and recombinant proteins		
Tetrodotoxin citrate	Tocris	1069; CAS: 18660-81-6
Dopamine hydrochloride	Sigma-Aldrich	H8502; CAS: 62-31-7
Forskolin	Sigma-Aldrich	F6886; CAS: 66575-29-9
Deposited data		
NeuPrint	Scheffer et al.[21] Plaza et al.[30]	https://neuprint.janelia.org/
FlyWire	Dorkenwald et al.[23] Schlegel et al.[24]	https://codex.flywire.ai/
Clock neurons single-cell sequencing data	Ma et al.[16]	GSE157504
Experimental models: Organisms/strains		
Drosophila melanogaster: Clk856-GAL4	Gummadova et al.[31]	BDSC_93198
Drosophila melanogaster: UAS-FRT-STOP-FRT-CsChrimson-mVenus	Wu et al.,[41]	N/A
Drosophila melanogaster: ITP-LexA	Deng et al.[32]	N/A
Drosophila melanogaster: LexAop-flippase	Bloomington Drosophila Stock Center	BDSC_55820
Drosophila melanogaster: UAS-EGFP	Bloomington Drosophila Stock Center	BDSC 5430
Drosophila melanogaster: ss00639-GAL4	Laboratory of Gerald Rubin	N/A
Drosophila melanogaster: MB122B-GAL4	Laboratory of Gerald Rubin	BDSC 88075
Drosophila melanogaster: UAS-CsChrimson-mVenus	Bloomington Drosophila Stock Center	BDSC 55134
Drosophila melanogaster: Trissin-LexA	Deng et al.[32]	N/A
Drosophila melanogaster: UAS-Kir2.1	Bloomington Drosophila Stock Center	BDSC 6596
Drosophila melanogaster: UAS-TNT	Bloomington Drosophila Stock Center	BDSC 28837
Drosophila melanogaster: UAS-Cas9.P2	Bloomington Drosophila Stock Center	BDSC 58985
Drosophila melanogaster: UAS-Dop1R1-guide	Schlichting et al.[29]	N/A
Drosophila melanogaster: UAS-Dcr-2	Bloomington Drosophila Stock Center	BDSC 24646
Drosophila melanogaster: UAS-Dop1R1-RNAi	Bloomington Drosophila Stock Center	BDSC 31765
Drosophila melanogaster: UAS-EPAC-H187	Laboratory of Michael Rosbash; Dr. Xihuimin Dai; unpublished	N/A
Drosophila melanogaster: 10XUAS-cAMPFIRE-M	Laboratory of Haining Zhong and Bing Ye; Dr. Elizabeth Cebul; unpublished	N/A

REAGENT or RESOURCE	SOURCE	IDENTIFIER
Drosophila melanogaster: UAS-GtACR1-YFP	Bloomington Drosophila Stock Center	BDSC 92983
Software and algorithms		
Neuprint	Scheffer et al.[21] Plaza et al.[30]	https://neuprint.janelia.org/
Flywire.ai	Dorkenwald et al.[23] Schlegel et al.[24]	RRID:SCR_019205
MATLAB R2022b	MATLAB	RRID:SCR_001622
Sleep and Circadian Analysis MATLAB Program	Vecsey et al.[62]	https://academics.skidmore.edu/blogs/cvecsey/?page_id=57
LAS X	Leica	RRID: SCR_013673
Microsoft Excel	Microsoft	RRID: SCR_016137
Fiji	Fiji	RRID:SCR_002285
Fly Sleep Probability	Wiggin et al.[40]	https://github.com/Griffith-Lab/Fly_Sleep_Probability
RStudio	Posit	RRID:SCR_000432
Seurat V3	Stuart and Butler et al.[63]	RRID:SCR_016341
Python Programming Language	https://www.python.org/	RRID:SCR_008394
Jupyter Notebook	https://jupyter.org/	RRID:SCR_018315
seaborn	https://seaborn.pydata.org/	RRID:SCR_018132